AMRL-TR-68-111

FEASIBILITY INVESTIGATIONS OF ELECTROSTATIC PRECIPITATION FOR THE REMOVAL OF GASEOUS TRACE CONTAMINANTS FROM MANNED CABIN ATMOSPHERES

GEORGE J. DOYLE

FOREWORD

This work was performed at the Southern California Laboratories of Stanford Research Institute, South Pasadena, California, 91030, under Contract No. AF 33(615)-2405 with Aerospace Medical Research Laboratories. The study was conducted in support of Project No. 6373, "Equipment for Life Support in Aerospace," Task No. 637302, "Respiratory Support Equipment." Work was monitored by Mr. William H. Toliver, Sr., Biotechnology Branch, Life Support Division, Biomedical Laboratory of the Aerospace Medical Research Laboratories, Wright-Patterson Air Force Base, Ohio. The period of performance by the Stanford Research Institute was from 1 November 1966 to 31 May 1968.

This study was under the specific direction of Dr. George J. Doyle, with contributions by Dr. R. G. Caldwell and Dr. C. J. Cook. General direction was afforded by Mr. L. P. Berriman. The research was under the administrative direction of Dr. R. D. Englert, Director, Scientific and Technical Operations, Southern California Laboratories. The author wishes to express his appreciation for the encouragement and assistance provided by Mr. W. H. Toliver, Sr.

This technical report has been reviewed and is approved.

WAYNE H. McCANDLESS
Technical Director
Biomedical Laboratory
Aerospace Medical Research Laboratories

ABSTRACT

This research is part of a program to study the feasibility of using a modified mode of electrostatic precipitation to remove polar gaseous trace contaminants from manned space-cabin atmospheres. A cell was developed for the removal of polar contaminant molecules from a 100 ml/min air inflow at part-per-million concentration levels of the contaminant. The operating principle of this cell is as follows: Positive lithium ions are thermionically generated and injected into the contaminated air stream. Ionic reaction products are collected at a set of porous metal collection electrodes. These electrodes are air-eluted. They are situated at the bottoms of slot-shaped wells to minimize escape of the collected contaminant molecules through diffusion. A measured efficiency of 20% for removal of acetone at a concentration of 1 ppm in dry air was finally achieved with this cell after considerable development work on the apparatus. This result is tentative pending further confirmatory experiments.

TABLE OF CONTENTS

TABLE OF CONTENTS (concluded)

LIST OF ILLUSTRATIONS

LIST OF TABLES

Section I

INTRODUCTION

A lightweight air purification unit of low energy consumption and long service life is needed for use on long duration space missions. New purification techniques for space cabin atmosphere would release the system design engineer from the constraints imposed by the present state of the art. One attractive possibility is to extend the technique of electrostatic precipitation to particles of molecular size. A feasibility study to demonstrate electrostatic precipitation of molecularly dispersed contaminants was undertaken because present knowledge does not justify initiation of a development program.

The first phase of this inquiry was a nonexperimental study to explore means for implementing the concept (Doyle and Caldwell, 1966). In that study, the consequences of injecting ions into a contaminated atmosphere and collecting the resultant charged species were considered on the basis of present knowledge. The pertinent conclusion was that injected ions, about which contaminant molecules cluster, offered the most promise for an experimental feasibility study.

Further consideration led to the selection of thermionically generated Li^+ (positive lithium ions) for the experimental phase. Positive ions were chosen because they tend to be smaller sized than negative ions, thus furnishing more intense local electric fields that increase the energy of interaction between ion and clustering molecule. The smallest alkali metal ion was chosen because of size consideration and because it has a low electron affinity. This low affinity reduces the likelihood of charge transfer to other molecules by fast bimolecular processes, such as $Li^+ + X \rightarrow Li + X^+$. (The low electron affinity does not exclude slower reactions, such as $Li^+ + 2H_2O \rightarrow LiOH + H_3O^+$, which is nearly thermoneutral; however, this particular reaction should have no net effect on the number of effective clustering ions.) The fact that techniques of thermionically generating Li^+ are well known was also a factor in this choice.

The nonexperimental study showed that small contaminant molecules having large permanent dipole movements have the largest energy of interaction with a small clustering ion. Such a polar molecule, acetone, was chosen as the first model contaminant, inasmuch as it was desirable to start with a favorable case and progress to less favorable cases. Another fact influencing this choice was that ketones are among the known contaminants in present space-cabin atmospheres.

Section II

SUMMARY

Ion Source Development

A major part of the experimental effort centered on development of a suitable source of thermionic lithium ions (Li^+). This ion source is required to operate in air at one atmosphere and to draw the least heating power practicable for heating the thermionic material, β-eucryptite, to 1000°C. Oxidation of the contaminant at or near the hot surface of the source must be minimized in order that this affect will not overwhelm effects due to electrostatic removal. The source also must be effectively distributed over an area of the order of 1000 cm^2 to avoid excessive polarizing potentials at the required current, about 10μa. The design developed to meet these specifications comprises a grid of ten parallel electrically heated, nickel-chromium alloy (Tophet A) wires (0.008-cm diameter by 27-cm long) coated with finely powdered (20μ or less particle size) β-eucryptite. Techniques for β-eucryptite preparation, wire treatment, and wire coating were developed that gave a coated wire capable of sustaining a positive-ion current of more than 0.02 μa/cm of length for four or more hours in air. Interruption of the heating power to the ion source resulted in nearly complete loss of ion emission on reheating. A single attempt to unequivocally identify the positive ion collected from the wires as lithium was inconclusive.

Major problems were encountered in mounting the fragile wires so as to obtain a reliable ion source grid within the cell. The hot wires tended to break under the pretensioning necessary to avoid sag due to thermal expansion. Breakage of the wire is attributed to loss of tensile strength at high temperatures compounded by the weakening effect of pitting corrosion during their service life. However, a tensioning system was devised that allowed sufficient reliability for use of one set of wires per experiment. Tensioning with two prestressed helical springs (20 turns by 0.5-cm diameter) made of 0.016-cm diameter nickel wires welded to the ends of each wire of the grid yielded fairly satisfactory reliability, provided no heating current passed through the spring.

Ion current from the source to the collecting electrodes was measured by a battery powered electrometer (Keithley Model 601) inserted into the ground-return lead of the polarizing power supply for these electrodes. The electrometer output was recorded on a potentiometer having an input circuit isolated from ground (Nesco DY110).

Experiments with Acetone as a Contaminant

The remainder of the effort under this contract was devoted to experimental determinations of the efficiency of the complete cell for removal of acetone from dry air containing 1 ppm of this contaminant. A hydrogen flame ionization detector (part of the Aerograph Model 600 GLC unit) was adapted to measure less than 1 ppm of acetone in air. The adapted apparatus uses only the flame ionization burner and ignition circuit of the Aerograph unit in conjunction with a 300-volt battery polarization supply and an electrometer (General Radio Model 1230A) to drive a recording potentiometer. An RC circuit at the electrometer input was chosen for a time constant of 100 sec, which gave adequate speed of response and a usable signal-to-noise ratio. Typically, one ppm of acetone at a 25 ml/min sampling rate gave 2.5×10^{-12} amp response against a background of 10^{-11} amp for a blank of 25 ml/min of pure carrier air. Some difficulties were encountered with sorption-desorption phenomena in various components of the flow system. These problems were more severe than those usually encountered in handling trace-concentrations because of the very low water vapor concentration in the carrier gas employed. Polar water molecules compete with the contaminant for sorption sites.

A typical experiment on acetone removal involved an influent flow rate of 100 ml/min of 1 ppm acetone in air and an effluent rate of 75 ml/min. The remaining 25 ml/min was withdrawn through the collection electrodes as an eluent enriched stream. Flame ionization analysis of the eluent stream at steady state (supplemented by occasional analysis of the influent mix) was used to ascertain the effect of passing positive ions from the source through the cell contents at currents of 3-10 μa (typically 5 μa). Efficiencies were calculated as the ratio of the observed steady state increase in acetone flux (ppm x ml/min) in the eluent stream on activating the ion source to the maximum flux increase that could be expected on the basis of one acetone molecule per 4.8×10^{-10} stat coulomb collected at the eluted electrodes. If the influx of acetone to the cell was exceeded by the flux corresponding to the ion current used, the acetone influx was used as the denominator to calculate an efficiency. One partially successful and two significant experiments indicated an efficiency of 20%. However, both blank and confirmatory runs must be carried out before complete confidence can be placed in these results.

There are reasons to believe that a second mode of cell operation, in which a separate stream of pure air is used to elute the collecting electrodes, would be more efficient. No meaningful trial in this mode has been carried out.

Section III

POSITIVE LITHIUM IONS FOR CLUSTERING

Suitability of Positive Lithium Ions

Clustering theoretically applies to a restricted class of contaminants (Doyle and Caldwell, 1966). However, the ion nucleus for the cluster and the conditions for cluster formation must be chosen so as to suppress competing reactions other than clustering by other polar molecules.

The ion nuclei must be sufficiently stable so that they will not undergo charge exchange or ion-molecule reaction at an appreciable rate, that is, the reaction half life should be long compared to the average time between ion generation and collection. A small ion is favorable for tightly bound structures. Of the two ions derivable from the same neutral species, the positive ion tends to be the smaller. Therefore, small positive ions such as H^+ (positive hydrogen), He^+ (positive helium), or Li^+ (positive lithium) are indicated for use in a feasibility test of clustering as a purification mechanism. However, the ionization potential of the "mother" atom should be low to avoid competition by electron-exchange reactions. This effectively rules out H^+ and He^+ ions.

An ion H_3O^+, derived from H^+, was considered in detail as a model cluster nucleus in the nonexperimental study by Doyle and Caldwell (1966). This ion is stabilized against electron exchange by the considerable proton affinity of water. The hydrated proton, H_3O^+, also has the favorable property of being energetically capable of charging some classes of contaminants by proton-exchange reactions with them (Vedene'ev et al., 1962, p. 211-214, Table 15; Munson, 1965, p. 5313). However, H_3O^+ is considerably larger than either H^+ or Li^+; a further disadvantage is that a still larger cluster centered on H^+ involving four water molecules has been predicted to be fairly stable (Doyle and Caldwell, 1966). Overall, it appears that Li^+ ions are comparable to, or even slightly better than, H_3O^+ for cluster formation by purely electrostatic forces, while lithium's ionization potential of 5.4 ev makes it immune to electron-exchange reactions.

The discussion of competitive clustering of different molecular species with H_3O^+ ions given by Doyle and Caldwell (1966) may be applied almost in its entirety to competitive clustering around Li^+ ions. The general conclusion that small polar molecules would preferentially cluster (rather than the larger, less polar molecules) remains applicable. In addition to the electrostatic and polarization effects in H_3O^+ ion clustering, it was pointed out that there may be additional effects due

to specific hydrogen-bonding effects, mobility of protons in a cluster, and rearrangement of clusters due to proton transfers. These possibilities, however, do not affect the application of the general treatment to clustering around Li^+ ions.

Data in Figure 1 of Doyle and Caldwell's report (1966), illustrate the electric field strengths around the H_3O^+ ion model used and allows us to compare the relative energies of clustering around Li^+ and H_3O^+ ions. The field strength is greatest along the symmetry axis of the ion on the hydrogen atom side of the ion, and weakest on the oxygen atom apex side of the ion. Since these are maximum and minimum values for the field strength at any given distance, the field strengths at intermediate orientations are intermediate.

Comparing the field strength of a Li^+ ion, approximated by a point charge at the origin, with that of the H_3O^+ ion reveals that the Li^+ ion field strength approximates that along the H_3O^+ ion's symmetry axis at distances of 2Å or more along the H_3O^+ ion axis. At other orientations, the field strengths around a Li^+ ion have higher positive values at any given distance. This means that, while the electrostatic binding of a first contaminant molecule that is within a certain distance of the ions might be comparable for binding the contaminant molecule to Li^+ and H_3O^+ ions, the spherical symmetry of the Li^+ ion favors addition of further molecules to the primary shell more than does the nonspherically symmetric field around the H_3O^+ ion. Further, the smaller size of the Li^+ ion favors increased electrostatic binding.

Margenau (1941, p. 603) has estimated the interaction energies between positive ions and neutral molecules. Interaction energies were estimated for Li^+ ions and a series of neutral molecules ranging in size from He to CO_2, using both induced dipolar and quadripolar polarization energies as well as van der Waal's energies; these energies ranged from 4-17 Kcal/mole.

Later workers estimated values about half of these (Munson and Hoselitz, 1939, p. 43). To estimate polar effects, we assumed a hypothetical dipole of strength $\mu = 1.5D$, a separation of charge of 2Å in the dipole, and a distance of closest nuclear approach to the Li^+ ion of 2.2Å. Using the methods discussed in the report, an electrostatic interaction of 11 Kcal/mole was estimated. The effect of adding an electrostatic term reinforced our previous conclusions on the importance of electrostatic effects. A value this large would increase the probability of collecting a polar contaminant molecule by a factor $\sim 10^8$.

On the whole (neglecting discussions of three-body effects, and the like) Li^+ ions seem to be favored over H_3O^+ ions for the formation of ion clusters. (The question of competitive clustering of different contaminant molecules is covered by our previous discussion.) Therefore, the experimental demonstration of feasibility of electrostatic purification was applied to clustering about Li^+ ions.

Generation of Positive Lithium Ions

A number of thermal methods for ion generation from alkali and alkali-earth metals have been published and offer apparent ready solutions to the practical problem of Li^+ ion generation. One method involves the contacting of alkali atoms with a hot surface of high work function (for example, oxide-covered tungsten), which results in electron exchange to yield positive alkali ions (Green, 1955, p. 85; McDaniel, 1964, p. 246-47; Massey and Burhop, 1952, p. 487; Rubin, Dittmer, and Benderson, 1964, p. 1720). This type of source should be avoided because of the need to prevent reaction of hot alkali vapor with the atmospheric constituents. Another method involves the thermionic emission of alkali ions from hot ion-containing compounds. The compounds most successfully used in this manner consist structurally of polymeric alumino-silicate negative ions held together by positive alkali ions (Rubin, Dittmer, and Benderson, 1964, p. 1720; McDaniel, 1964, p. 461, 683-85; Massey and Burhop, 1952; p. 486; Blewett and Jones, 1936, p. 464; Cropton and Elford, 1959, p. 497; Allison and Kamegai, 1961, p. 1090) although oxides (McDaniel, 1964, p. 461, 683-85; Blewitt and Jones, 1936, p. 464) have been used. (Possibly the Kunsman sources [Massey and Burhop, 1952, p. 487] can also be placed in this class of ion sources.) The anticipated problems with these sources were chemical attack on the supporting filaments by atmospheric constituents; undesirable chemical reactions on the hot surface (about 1000°C [Blewett and Jones, 1936, p. 464]); and space-charge effects, particularly near the source.

Section IV

MATHEMATICAL MODEL USED IN DESIGNING PURIFICATION CELL

Differential Equations and Their Solution

To provide a basis for design of the purification cell, it was necessary to generate approximate equations by devising a simplified mathematical description of processes occurring within such a cell. The simple treatment given by Doyle and Caldwell (1966) was not suitable because the mobilities of the reactant and the product ion differ so markedly (see below). In our first attempt to solve this more complex problem, the effect of diffusion was neglected and a concurrent flow of reagent ion and of contaminated atmosphere (one contaminant) was assumed. Atmosphere flow velocity was assumed negligible in comparison with ionic drift velocities in the reaction zone. These assumptions resulted in a set of four simultaneous differential equations for the steady state situation:

$$-kn_1n_o - K_1 \frac{d}{dx}(n_1E) = 0 \qquad (1)$$

$$+kn_1n_o - K_2 \frac{d}{dx}(n_2E) = 0 \qquad (2)$$

$$-kn_1n_o - v\frac{dn_o}{dx} = 0 \qquad (3)$$

$$-4\pi e(n_1 + n_2) + \frac{dE}{dx} = 0 \qquad (4)$$

where n_o = molecular concentration, cm^{-3} of unreacted contaminant (for example, acetone)
n_1 = concentration of reagent ion, cm^{-3} (for example, Li^+)
n_2 = concentration of complex ion, cm^{-3} (for example, $[Li^+(CH_3)_2CO]$)
k = second-order rate constant for the complexing reaction, cm^3/sec
K_1 = mobility of reagent ion
K_2 = mobility of complex ion
E = field strength, esu
v = linear flow velocity of the contaminated atmosphere, cm/sec
x = coordinate, cm
e = electronic charge esu

Equations (1) to (3) represent the consequences of conservation of matter and Eq (4) is Poisson's equation for a unidimensional field and charge distribution. These equations are implicitly soluble in terms of elementary transcendental functions. The first step was to establish two integrals of the system. Eqs (1) and (2) were added and integrated to obtain

$$e(K_1 n_1 + K_2 n_2)E = j \tag{5}$$

where j = current density, stat amperes/cm^2, a constant at steady state. Eqs (2) and (3) were added and integrated to obtain

$$K_2 n_2 E + v n_o = \ell \tag{6}$$

where ℓ = flow of bound and unbound acetone per unit electrode area, cm^{-2} sec^{-1}, a constant at steady state which also can be set equal to $(n_o)_{x=o}v$. These constants of the system were combined with Eqs (1) to (4) to reduce the set of four equations to two:

$$E\frac{d(n_2E)}{dx} = \left[\frac{kj}{K_1K_2e} - \frac{k}{K_1}(n_2E)\right]\left[\frac{\ell}{v} - \frac{K_2}{v}(n_2E)\right] \tag{7}$$

$$E\frac{dE}{dx} = \frac{4\pi j}{K_1} + 4\pi e\frac{K_1 - K_2}{K_1}(n_2E) \tag{8}$$

The forms of Eqs (7) and (8) suggested an integration giving (n_2E) as a function of E. In doing this it was convenient to introduce dimensionless variables and parameters to give

$$\frac{d\psi}{d\xi} = \frac{(1 - \beta\psi)(1 - \psi)}{(1 + \alpha\beta\psi)} \tag{9}$$

where $\psi = K_2(n_2E)/\ell$
$\xi = kE/4\pi ev$
$\alpha = K_1 - K_2/K_2$
$\beta = e\ell/j$

One should note that, for cocurrent ion and contaminant flux, ψ is the fraction of contaminant present as the complex ion and β is the reciprocal of the ratio of reagent ion to the contaminant's flow rates. Integration of Eq (9) leads to

$$\xi - \xi_o = \left[\frac{1}{1-\beta} + \frac{\alpha}{2}\frac{1+\beta}{1-\beta}\right] \ell n \left[\frac{1-\psi\beta}{1-\psi}\right] + \left[\frac{\alpha}{2}\right] \ell n \left[(1-\beta\psi)(1-\psi)\right] \qquad (10)$$

The boundary condition $\psi = 0$ for $\xi = \xi_o$ has been applied in Eq (10). Introduction of a dimensionless coordinate, $\eta = k^2 \ell \alpha x / 4\pi K_1 e v^2$, into Eq (8) allows one to write

$$\eta = \xi_o \int_o^{\psi} \frac{\left(\frac{d\xi}{d\psi}\right)_{\psi=t} dt}{\frac{1}{\alpha\beta} + t} + \int_o^{\psi} \frac{\left[(\xi-\xi_o)\frac{d\xi}{d\psi}\right]_{\psi=t} dt}{\frac{1}{\alpha\beta} + t} \qquad (11)$$

which, on integrating by parts to eliminate $(d\xi/d\psi)_{\xi=t}$, gives

$$\eta = \xi_o \left\{ \frac{\xi(t)-\xi_o}{\frac{1}{\alpha\beta} + t} \Bigg|_o^{\psi} + \int_o^{\psi} \frac{\xi(t)dt}{\left(\frac{1}{\alpha\beta} + t\right)^2} \right\} + \tfrac{1}{2} \left\{ \frac{\left[\xi(t)-\xi_o\right]^2}{\frac{1}{\alpha\beta} + t} \Bigg|_o^{\psi} + \int_o^{\psi} \frac{\left[\xi(t)-\xi_o\right]^2}{\left[\frac{1}{\alpha\beta} + t\right]^2} dt \right\} \qquad (12)$$

which, with Eq (10), allowed us to calculate corresponding values of $\psi (o \leq \psi < 1)$, η, and ξ, given ξ_o, α, and β.

Evaluation of Parameters of the Equations

These equations yielded a first approximation to such things as purifier dimensions, current density, and collecting potentials. In evaluating parameters, one of the more important was the reaction rate of contaminant molecules with the injected lithium ion. This was estimated by classical reasoning using the equation

$$k = \pi r^3 \left(v_A^2 + v_L^2\right)^{\frac{1}{2}} \left(\frac{1}{\lambda_A} + \frac{1}{\lambda_L}\right) \tag{13}$$

where k = specific second-order rate constant, cm^3/sec, for clustering in the presence of a great excess of carrier gas, whose influence is taken into account by means of the mean free paths of the molecule λ_A and of the ion λ_L

v_A = mean speed of the molecules

v_2 = mean speed of the ions

r_1 = an ion-to-molecule distance, within which an orbiting collision between them occurs

The physical concept (McDaniel, 1964, p. 71-75, 571-74) is as follows: During an orbiting collision, potential energy of the system ion-molecule is converted to kinetic energy or rotation; if during this binary collision event a third collision with a carrier gas molecule occurs, nearly all such tertiary collision will reduce the kinetic energy of the rotating pair sufficiently to irreversibly initiate equilibration of the "hot" clusters toward the average thermal energy of the bulk gas, thus stabilizing them against dissociation. This radius was estimated by the equation

$$r_1 = \left(\frac{\alpha e^2}{3kT}\right)^{\frac{1}{4}} \tag{14}$$

where α = molecular polarizability, cm^3

e = electronic charge (esu)

k = Boltzman constant

T = absolute temperature

The polarizability was estimated by the equation

$$\alpha = \frac{K-1}{4\pi N} \tag{15}$$

where K = dielectric constant of the pure gas (of the contaminant at a molecular concentration N cm^{-3}). The mean speeds were calculated by the usual classic expressions $v = 2/\sqrt{\pi}\,\beta$, $\beta = (m/2kT)^{\frac{1}{2}}$ (m = molecular or ionic mass, gm). The molecular mean free path λ_A was calculated by the expression

$$\lambda_A = \frac{1}{n_2 S_{12}\left[1 + \left(\frac{m_1}{m_2}\right)^2\right]^{\frac{1}{2}}} \tag{16}$$

$$\lambda_L = \frac{1}{n_2 q} \tag{17}$$

where q = cross section for collision, which may be adequately approximated for the present purposes by the equation for orbiting cross section

$$q = \frac{2\pi}{v_o}\left(\frac{e^2\alpha}{M_r}\right)^{\frac{1}{2}} \tag{18}$$

where v_o = the mean speed of carrier gas molecules
α = molecular polarizability of carrier gas
M = the reduced mass of the colliding molecules (for example, Li^+ and O_2)

The reaction rate was numerically estimated for Li^+ in O_2 reacting with trace amounts of acetone. With the above substitution, the equation for the specific rate simplifies to

$$k = \frac{\pi^{\frac{1}{2}} r_1^3 2^{\frac{3}{2}} (kT)^{\frac{1}{2}}}{M_r^{\frac{1}{2}}}\left(\frac{1}{\lambda_A} + \frac{1}{\lambda_L}\right) \tag{19}$$

and, using the values

$r_1 = 1.86 \times 10^{-7}$ cm (K = 1.0159 at N = 1.97×10^{19})
$\lambda_A = 3.5 \times 10^{-6}$ (acetone in oxygen)
$\lambda_L = 2.6 \times 10^{-6}$ (Li^+ in oxygen)

one obtains

$$k \sim 7.2 \times 10^{-11} \text{ cm}^3/\text{sec} \tag{20}$$

The assumption that $k \sim 10^{-10}$ cm^3/sec seems fairly safe.

For the above calculated constant (Eq 20) to give a good estimate of reaction rate, the contaminant, ion, and cluster concentrations must be far from satisfying the equilibrium relationship

$$K = \frac{n_{LA}}{n_L n_A} \tag{21}$$

during the greater part of the residence time in the reactor. It was therefore necessary to estimate the value of K. Additional information from the values of K and k were estimates of the rate of cluster dissociation or the mean lifetime of a cluster, which should be greater than the residence time of an ion between the electrodes to ensure efficient removal of the contaminant. K was estimated by standard statistical thermodynamic principles (Doyle and Caldwell, 1966). Thus,

$$K = e^{-\frac{\epsilon_o}{kT}} \xi_T \xi_V \xi_R \tag{22}$$

taking

$$\xi_T = \frac{k^3}{(2\pi kT)^{\frac{3}{2}}} \frac{1}{\mu^{\frac{3}{2}}} \tag{23}$$

(μ = reduced mass of reaction partners)

$$\xi_V = \frac{1}{2 \sinh (h\nu/2kT)} \tag{24}$$

$$\xi_R \simeq \left[\left(I_1 I_2 I_3\right)_{LA} \Big/ \left(I_1 I_2 I_3\right)_{A} \right]^{\frac{1}{2}} \tag{25}$$

as the partition function quotients. Values taken for the parameters were estimated by straightforward methods. The principal moments of inertia for the cluster (I_1, I_2, and I_3) were estimated by assuming an undistorted acetone molecule with its center of mass 3.6Å from the Li^+ ion along a rotational symmetry axis of the $>C{=}O$ bond. The fundamental frequency ν was taken as 6×10^{12} sec^{-1}. The results were $\xi_T = 6.6 \times 10^{-26}$, $\xi_V = 1.00$, $\xi_R = 2.4$, thus giving

$$K = 1.6 \times 10^{-25} \, e^{-\frac{\epsilon_o}{kT}} \, cm^3 \tag{26}$$

For 6.02×10^{23} $\epsilon_o \sim 35$ Kcal/mole, Eq (26) yielded

$$K \sim 5.1 \, cm^3 \tag{27}$$

Concentration levels for the proposed experiments were ionic concentration of 10^8 cm^{-3} and acetone concentrations ranging downward from 10^{13} cm^{-3} as the reaction progressed. The most unfavorable situation one can conceive for unclustered acetone is embodied in the equations

$$n_L + n_{LA} = 10^8 \, cm^{-3} \tag{28}$$

and

$$n_A = n_L \tag{29}$$

giving, at equilibrium, $n_A \simeq 10^4$ for K = 5. The situation envisaged in the experimental plan (see below) was a twofold excess of ions at termination of reaction

$$n_L + n_{LA} = 2(n_A + n_{LA}) \sim 10^8 \tag{30}$$

giving, at equilibrium,

$$n_A \sim 0.4 \, cm^{-3} \tag{31}$$

Since the calculations were based on only 50% efficiency of removal (see below), the concentrations are far removed from equilibrium at termination (provided the estimate of k is correct) and the assumption of a second-order reaction mechanism is still valid. The cluster dissociation rate, by the principle of detailed balancing, is

$$k_r = k/K \sim 10^{-11} \text{ sec}^{-1} \tag{32}$$

given an average life 10^{11} sec, which is much greater than the residence time of an ion ($\sim 10^{-3}$ sec).

The mobility of Li^+ ion was taken as $K_1 = 1180$ esu (McDaniel, 1964, p. 481). The mobility of the complex ions, K_2, was calculated using the Langevin-Hasse equation (McDaniel, 1964, p. 431-34) for the specific case of an acetone-Li^+ complex ion. This equation involves the radius of the complex ion, which was estimated from the viscosity derived kinetic theory (Kennard, 1938, p. 135-205) radius of acetone, 3.51Å, plus a small correction for the attached Li^+ ion (based on the model used in the equilibrium constant calculation--see above) to give a radius of 3.53Å. Assuming a bimolecular carrier gas, such as oxygen or nitrogen at one atmosphere pressure, gives the value $K_2 = 226$ esu.

Numerical Results and Their Design Implications

These mobility values yield a value of 4.2 for the parameter α. The parameter β is set equal to 0.5 because a twofold excess of ion current over contaminant influx was envisaged for design purposes. This was not entirely an arbitrary decision. It was obvious that some excess must be present for the reactor interelectrode spacing to be finite. Values of ξ and η as a function of ψ are shown in Table I for various anode field strengths, ξ_o, for concurrent ion and contaminated atmosphere flow.

To avoid excessive field energy of an ion, the condition

$$\left(\frac{m_2}{m_1} + \frac{m_1}{m_2}\right) e\ E\ \lambda << k\ T \tag{33}$$

must be satisfied (McDaniel, 1964, p. 427).

Table I

DIMENSIONLESS FIELD STRENGTH, ξ, AND INTERELECTRODE SEPARATION, η, AS A FUNCTION OF FRACTION CONVERTED, ψ, FOR $\alpha = 4.2$, $\beta = 0.5$, AND FOR VARIOUS DIMENSIONLESS ANODE FIELD STRENGTHS ξ_o
(Concurrent Ion and Atmosphere Flow)

	$\xi_o = 0.0200$		$\xi_o = 0.070$		$\xi_o = 0.200$		$\xi_o = 0.70$		$\xi_o = 2.00$		$\xi_o = 7.0$		$\xi_o = 20.0$	
ψ	ξ	η	ξ	η	ξ	η	ξ	η	ξ	η	ξ	η	ξ	η
0.00	0.0200	0.00	0.070	0.00	0.200	0.00	0.700	0.00	2.00	0.00	7.00	0.00	20.0	0.00
0.05	0.0748	0.00516	0.125	0.0106	0.255	0.0248	0.755	0.0794	2.05	0.221	7.05	0.767	20.0	2.19
0.10	0.128	0.0150	0.178	0.0253	0.308	0.0521	0.808	0.155	2.11	0.423	7.11	1.45	20.1	4.13
0.15	0.217	0.0404	0.267	0.0581	0.397	0.104	0.897	0.281	2.20	0.740	7.20	2.51	20.2	7.10
0.20	0.308	0.0770	0.358	0.102	0.488	0.166	0.988	0.412	2.29	1.05	7.29	3.52	20.3	9.92
0.25	0.413	0.131	0.557	0.163	0.593	0.247	1.09	0.569	2.39	1.40	7.39	4.62	20.4	13.0
0.30	0.542	0.213	0.592	0.253	0.722	0.359	1.22	0.766	2.52	1.82	7.52	5.89	20.5	16.5
0.35	0.690	0.326	0.740	0.376	0.870	0.506	1.37	1.00	2.67	2.30	7.67	7.30	20.7	20.3
0.40	0.866	0.490	0.916	0.557	1.04	0.731	1.54	1.40	2.84	3.15	7.84	9.86	20.8	27.3
0.45	1.07	0.711	1.12	0.783	1.25	0.970	1.75	1.69	3.05	3.56	8.05	10.7	21.0	29.4
0.50	1.32	1.03	1.37	1.11	1.50	1.33	2.00	2.18	3.30	4.39	8.30	12.9	21.3	35.0
0.55	1.62	1.47	1.67	1.56	1.80	1.82	2.30	2.80	3.60	5.34	8.60	15.1	21.6	40.6
0.60	1.99	2.10	2.04	2.21	2.17	2.50	2.67	3.61	3.97	6.49	8.97	17.6	22.0	46.4
0.65	2.44	3.00	2.49	3.14	2.62	3.50	3.12	4.88	4.42	8.46	9.42	22.2	22.4	58.1
0.70	3.00	4.34	3.05	4.50	3.18	4.92	3.68	6.54	4.98	10.8	9.98	27.0	23.0	69.2
0.75	3.72	6.36	3.78	6.55	3.90	7.05	4.40	8.97	5.70	14.0	10.7	33.2	23.7	83.2
0.80	4.68	9.58	4.74	9.82	4.86	10.4	5.36	12.7	6.66	18.7	11.7	41.8	24.7	102.
0.85	6.02	15.1	6.08	15.4	6.20	16.1	6.70	18.9	8.00	26.3	13.0	54.5	26.0	128.
0.90	8.08	25.8	8.13	26.2	8.26	27.1	8.76	30.7	10.0	40.0	15.0	75.8	28.0	169.

Here m_2 = mass of carrier gas molecule
m_1 = ionic mass
E = field strength (esu)
λ = mean free path of the ion, which has already been estimated for Li^+ in O_2 as 2.6×10^{-6} cm

The numerical substitutions for the Li^+ ion led to the requirement that

$$E << 13 \text{ stat volt/cm} \tag{34}$$

Since the acetone-Li^+ ion cluster is stable by approximately 30 Kcal/mole, it was concluded that the reaction with acetone would not be greatly inhibited if

$$E \sim 1 \text{ stat volt/cm} \tag{35}$$

for the initial experiments. The mean free path and mass ratios for the complex ion are less than those for the Li^+ ion; consequently, for the same field strength the field energy of the complex is less than that of the Li^+ ion.

If the upper limit of 1 esu is chosen for the field strength and a reaction constant of $k = 10^{-10}$ cm^3/sec assumed (see Eq 20), then, for a given desired conversion ψ, one can write $4\pi ev\xi/k = 1$. Hence, $v = k/4\pi e\xi$ and $x = 4\pi K_1 ev^2\eta/k^2\ell\alpha = 4\pi K_1 ev\eta/k^2\alpha(n_o)_{x=o}$, allowing one to calculate v and, hence, the interelectrode separation required for the value of ψ, given $(n_o)_{x=o}$, the contaminant concentration in the influent atmosphere. One can also calculate 1/v, the electrode area required per unit inflow rate, and current density, $j = 2(n_o)_{x=o}ve$, for various electrode separations. This was done for $\psi = 0.5$ and 0.8, assuming a contaminant concentration of 1 ppm by volume $\left[(n_o)_{x=o} = 2.5 \times 10^{13} \text{ cm}^{-3}\right]$; results are shown in Table II and Figure 1.

It was evident from data in Figure 1 that a practical compromise would have to be struck between electrode area and electrode separation: Too small an electrode separation requires impractically high precision of construction accompanied by a small electrode area; a large separation demands impractically large electrode areas. The actual choice was aided by consideration of residence times in the reactor, which should not be unduly long to avoid excessively long times to reach steady state, as well as the occurrence of other probable processes of acetone removal, which would mask the desired effect and thus confuse interpretation of the experimental data.

Table II

OPERATING CONDITIONS OF A LABORATORY-SCALE PURIFIER FOR AN ATMOSPHERE CONTAINING 1 PPM OF CONTAMINANT ($\alpha = 4.2$, $\beta = 0.5$, $k = 10^{-10}$ cm^3/sec, $E \leq 1$ stat volt/cm)

Percent Conversion (100ψ)	Anode Field Strength (stat volt/cm)	Interelectrode Separation (cm)	Current Density (stat amp/cm^2)	Electrode Area per Unit Flow Rate of Atmosphere (sec/cm)	Residence Time of Atmosphere in Reactor (sec)
50	0.0151	0.087	300	80	7.0
	.051	.091	290	82	7.5
	.133	.100	264	90	9.1
	.348	.122	199	121	14.7
	.606	.150	120	200	30
	.840	.175	48	500	88
	.935	.186	19	1280	238
80	0.00427	0.230	85	282	65
	.0148	.234	84	285	67
	.0411	.242	82	293	71
	.130	.268	74	324	79
	.300	.316	60	402	127
	.600	.405	34	700	283
	.812	.464	16	1490	690

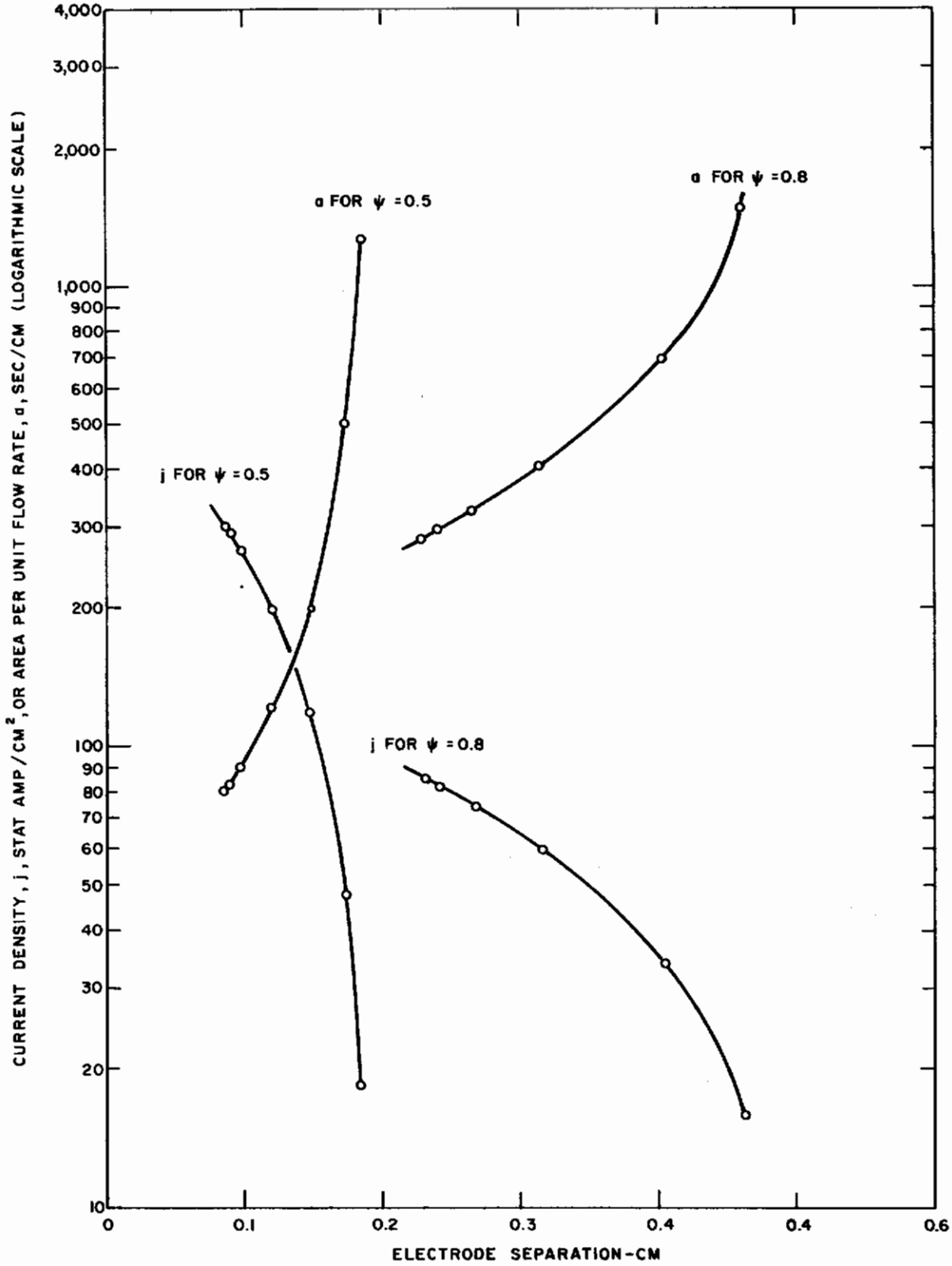

Figure 1. Current Densities and Areas per Unit Flow Rate Plotted Against Electrode Separation for Two Fractions Converted and for the Condition that Field Strength be Everywhere Less than or Equal to One Stat Volt/CM

Note that only cocurrent flow was considered in obtaining numerical data using the derived equations. The final design described below utilizes countercurrent flow to drive the ion-contaminant reaction further towards completion and to minimize exposure of influent contaminant to the neighborhood of the hot ion-source grid. This discrepancy between design equations and design, imposed by the sequence of events during this project, was not regarded as seriously affecting conclusions on apparatus design at the level of approximation prevailing in this initial effort. To consider the countercurrent case in detail, one need only consider the effect of negative air velocities v. This consideration changes the interpretation of the integral ℓ to the negative of residual acetone flux in the purified airflow/cm^2 of cell area. The dimensionless variables ψ become negative and the parameter β is also negative (and equal to -0.25 for the specific case of 50% efficiency and twofold excess of ionic current.) Figure 2 shows values of fraction complexed as a function of ξ for both the counter- and cocurrent mode. The countercurrent mode is only slightly superior.

Modification of Ideal Design

The ideal cell design implied by these theoretical considerations had to be modified so that the cell could satisfy two additional sets of requirements: those imposed by (1) measures necessary to suppress back diffusion of deposited contaminant from the collection electrode and (2) ion source design criteria. The latter calls for measures to suppress pyrolysis and oxidation of the contaminant by the hot source as well as attainment of a smooth joining of the radial fields about the ion source grid to the approximately unidimensional field in the neighborhood of the collecting electrodes.

A simple unidimensional steady state convective diffusion model with various boundary conditions was used to discover important cell design details affecting back diffusion of deposited contaminant. In general, a large value of the dimensionless parameter $v\ell/D$ is desirable when the eluting velocity v cm/sec opposes back diffusion of a contaminant of diffusion constant D cm^2/sec through a length ℓ, cm. However, diffusion lengths cannot be much greater than 1 cm because they are restricted by the requirement of small interelectrode separation (see above) for reasonable cell areas and collecting electric fields. The velocity v can be made large for a given volume flow rate by decreasing the electrode area. One must then accept as a penalty an increased collecting electric field for a given ion current. This was the direction taken to suppress diffusion--holding electrode separation roughly constant at 1 cm while decreasing electrode area and increasing electrode potentials. An electrode area of 100 cm^2 was found suitable in combination with diffusion lengths of 1 cm and eluting flow rates of tens of cubic centimeters per minute.

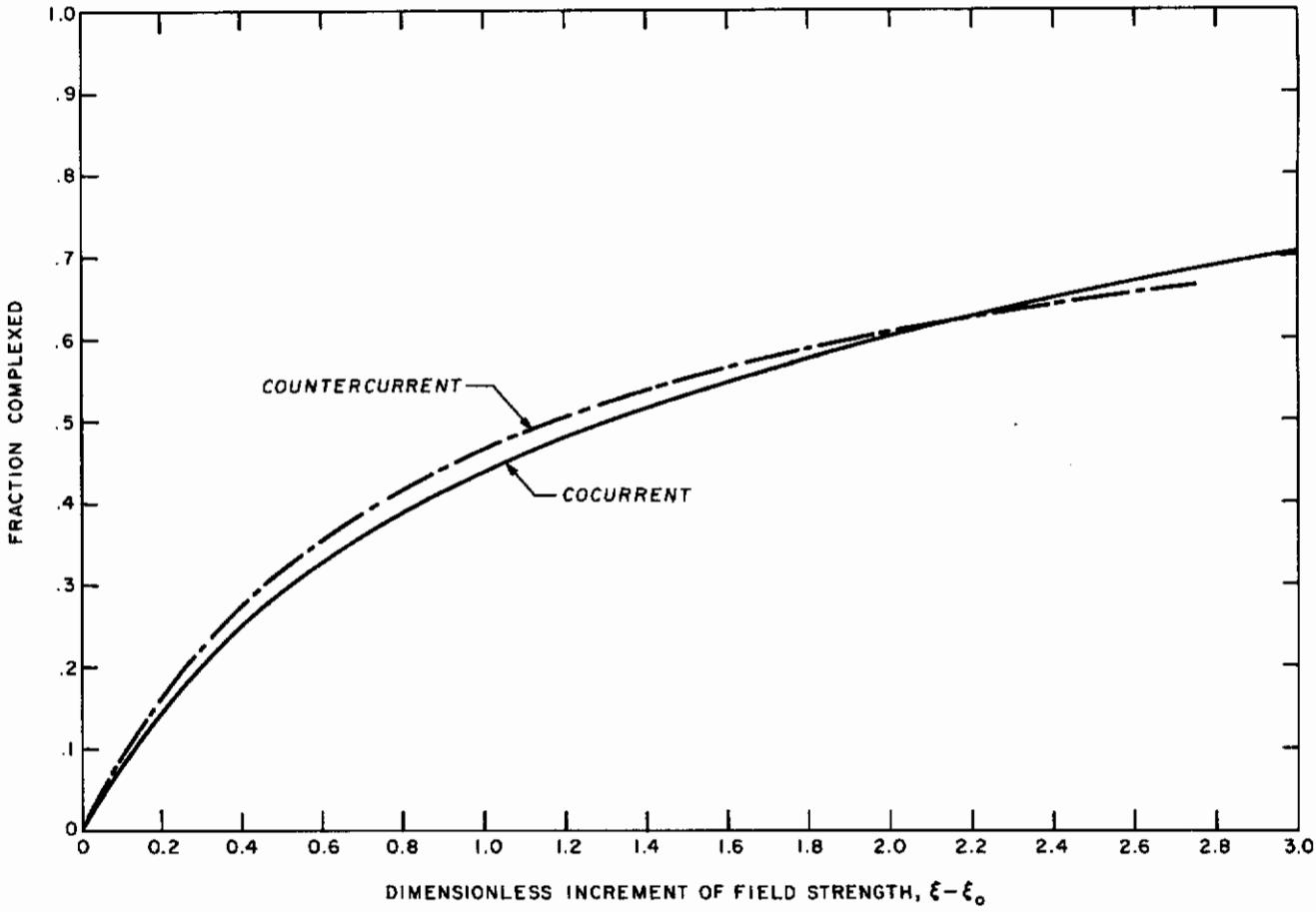

Figure 2. Fraction Complexed as a Function of Field Strength

The electrode design tentatively chosen to meet the above requirements consists of slots cut 1 cm deep in an insulating material and oriented parallel to the ion source grid (see below). At the bottom of these slots is the porous collecting surface, constructed of sintered stainless steel mesh and backed by galleries to collect the contaminant-rich stream. The influent contaminated stream is injected into the slots at a plane 0.5 cm away from the collecting surface. This stream flows countercurrent to the ion flux within the slot and then flows to an array of collection points on the surface of the insulating material situated halfway between the slots. An eluent stream, when used, is injected within the slots and at a plane slightly above the collecting surface. Guide electrodes at a positive potential lie between the strips of collecting surface. The solution to the one-dimensional convective diffusion differential equation for these boundary conditions is

$$C_e = \frac{C_o}{1 + \frac{v_1}{v_2} + \frac{v_1(\ell_2-\ell_1)}{D}} + \frac{S}{v_1}\left[1 - \frac{\exp(-v_1\ell_1/D)}{1 + \frac{v_1}{v_2} + \frac{v_1(\ell_2-\ell_1)}{D}} - \frac{\exp\left(-v_2(\ell_3-\ell_2)/D\right)}{1 + \frac{v_2}{v_1} + \frac{v_2(\ell_2-\ell_2)}{D}}\right] \quad (36)$$

where c_e = concentration in the enriched stream,
c_o = concentration in the influent stream
v_1 = eluent velocity field strength
v_2 = influent velocity field strength
$\ell_2 - \ell_1$ = diffusion length separating influent and eluent injection planes
D = diffusion constant of the contaminant in air
S = deposition rate per square centimeter of collecting area
ℓ_1 = length of eluent velocity field
$\ell_3 - \ell_2$ = length of influent velocity field

Using the proposed flow rates and collection area, this formula indicates that air efficiency up to 15% (30% of the maximum theoretical efficiency of 50%) can be attained at high eluent flow rates. As the entire design philosophy of the purifier and the associated calculations have been conservative, one can reasonably expect considerably better efficiencies than those calculated.

Section V

THE ION SOURCE

Emissivity of β-Eucryptite

The mechanism chosen to produce Li^+ ions is thermionic emission at 1000°C from β-eucryptite, a lithium alumino-silicate mineral that can be made synthetically (Allison and Kamegai, 1961, p. 1090). The experimentally found emission is said to follow an equation of the Richardson-Dushman type:

$$J = AT^2 \exp\left[-\phi/kT\right] \tag{37}$$

It is dubious that Schottky's modification of this equation, which takes into account the effect of field strength on the emission, is applicable inasmuch as hopping the surface potential barrier probably is not the rate-determining step. Using Blewett and Jones' finding (as quoted by Allison and Kamegai) that $J = 1$ ma/cm^2 for $T = 1409$°K, $j = 0.1$ ma/cm^2 for $T = 1319$°K, yields $J = 10^{14}\ T^2 \exp\left[-6.16\times10^{-12}/kT\right] \frac{\text{stat amp}}{\text{cm}^2}$ as the approximate expression for emission as a function of temperature.

Ion Current Field Near the Source

Our previous considerations showed that we needed an approximation to an ion source whose emission was distributed over a virtual planar electrode. Because of the high temperature required for emission, it was obviously necessary to minimize mass- and heat-transfer areas associated with the source. This pointed to an ion source consisting of a planar grid of closely spaced, fine wire sources furnished with the minimum power needed to sustain the required current density.

From Poisson's law it can be shown that the cylindrically symmetrical field at a distance r from such a wire is given by

$$\frac{E}{E_o} = \sqrt{\frac{4\pi r_o j_o}{K_1 E_o^2}\left(1 - \frac{r_o^2}{r^2}\right) + \frac{r_o^2}{r^2}} \tag{38}$$

where

$$j_o = J - \frac{ec_o}{2\sqrt{\pi}} \sqrt{\frac{2kT}{m}} = ec_o E_o K_1$$

$$r_o j_o = rj$$

and

$$j = ecEK_1 \tag{39}$$

Here E_o = field strength at the wire surface
r_o = radius of wire
j_o = current density at the wire surface
K_1 = Li^+ ion mobility, cm^2/volt x sec (esu)
J = emission density from wire, amp/cm^3 (esu)
c_o = ion concentration at the wire, cm^{-3}
m = ionic mass, gm.

These equations involve the implicit assumption that every ion colliding with the wire is resorbed (100% sticking probability).

Specifications Imposed on Ion Source

To join this field and current smoothly onto a unidimensional field near the collecting electrode, the grid was displaced from the virtual anode of the interelectrode field by a distance equal to one half of the grid spacing, thus increasing the distance between physical electrodes. Presuming that a third repellant electrode placed some distance behind the grid would suffice to drive all current to the cathode, the two fields were joined by the intuitive (and approximate) requirement that

$$2\pi R\, j(R) = 2Rj_a \tag{40}$$

$$2\pi R\, E(R) = 2RE_a \tag{41}$$

where R is one half of the grid spacing and the subscripts "a" refer to the requirements at the virtual anode. The value of r_o is the minimum value consistent with mechanical strength in order to reduce power needed to generate the ions. It was therefore a fair assumption that $R >> r_o$. The joining conditions and the equations of a cylindrical space-charge field then yielded the requirement that $E_a > 2\pi\sqrt{\frac{Rj_a}{K_1}} > 0$ in order that $E_o > 0$.

This lower limit for E_a is shown plotted as a function of j_a for various values of R in Figure 3. Also shown in Figure 3 are values of anode voltages plotted versus current density taken from Table II. As values of R less than 0.1 cm are impractical, values of current density greater than about 100 esu and of anode field strength less than about 0.4 esu cannot be practically attained in a laboratory test apparatus with this type of ion source. $\psi = 0.5$, $E_a = 0.67$, $j_a = 100$, and R = 0.1 seemed to be a good choice for an initial trial solution, since it represented a relatively high reactor current density. This choice gave an 0.155-cm separation between cathode and virtual anode and an electrode area per unit flow rate of 225 cm^2 (see Figure 1).

A tentative choice of grid wire size was B&S #40 Tophet A* covered with a thin film of β-eucryptite. This made $r_o = 0.004$ cm. The choice of E_a and j_a imposed the condition that $E_o = 2.74$ esu, $j_o = 795$ esu, and $Ec_o = 0.234$ esu. These values required, in turn, that the emission from the wire be

$$J = 795 + 3.22 \times 10^2 T^{\frac{1}{2}} \qquad (42)$$

where T = effective absolute temperature in the gaseous layer near the wire. Thus the required emission was between 6,400 and 11,400 amp/cm^2 (esu); $300 < T < 1{,}000°K$. The maximum emission is about 1 ma/cm^2 or 3×10^6 amp/cm^2 (esu), so there should be ample available emission intensity.

Figure 4 shows a graphic computation of the minimum wire temperature required, 1200°Å or 930°C. To achieve this temperature, 0.68 amp/grid wire is required and would give a power density of 5.5 watts/cm^2. The resultant heating power of 1.1 kw per unit flow rate distributed over 225 cm^2 would result in an unmanageable temperature control problem. A second trial solution must be chosen.

The simplest expedient to reduce heating power density was to decrease ion current density. This, of course, increased reactor size and contaminant residence time. We chose $\psi = 0.5$, R = 1, $j_a = 19$, and $E_a = 0.94$ as representing a practical low-current density operating condition (see Figure 3). We obtained an electrode separation of 0.19 and area per unit flow rate of 1,280 cm^2 (see Figure 1). The ion source in this case would be a grid of

---

* Trademark registered.

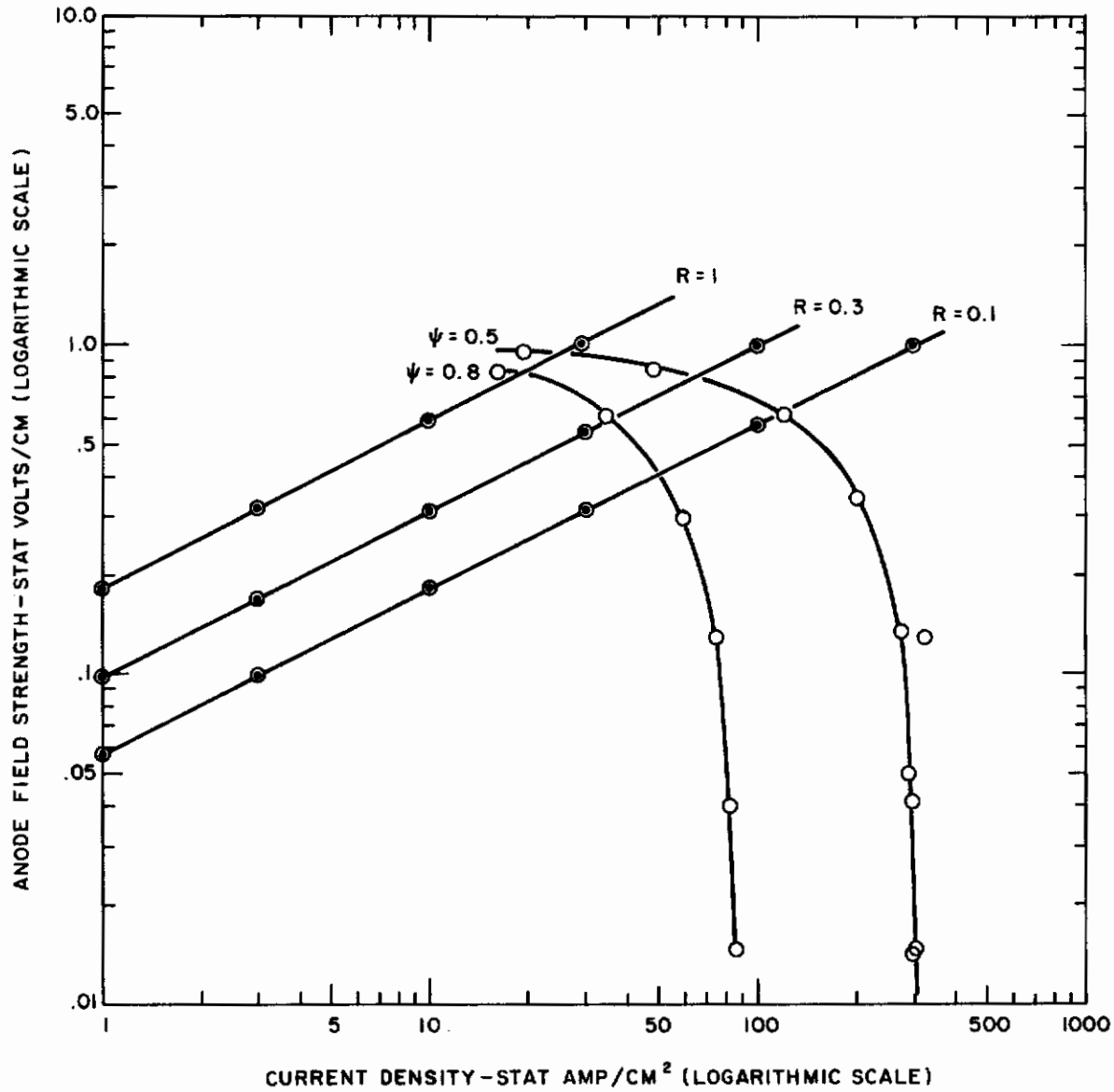

Figure 3. Graphic Aid for Choice of Grid Spacing R and of Interelectrode Geometry

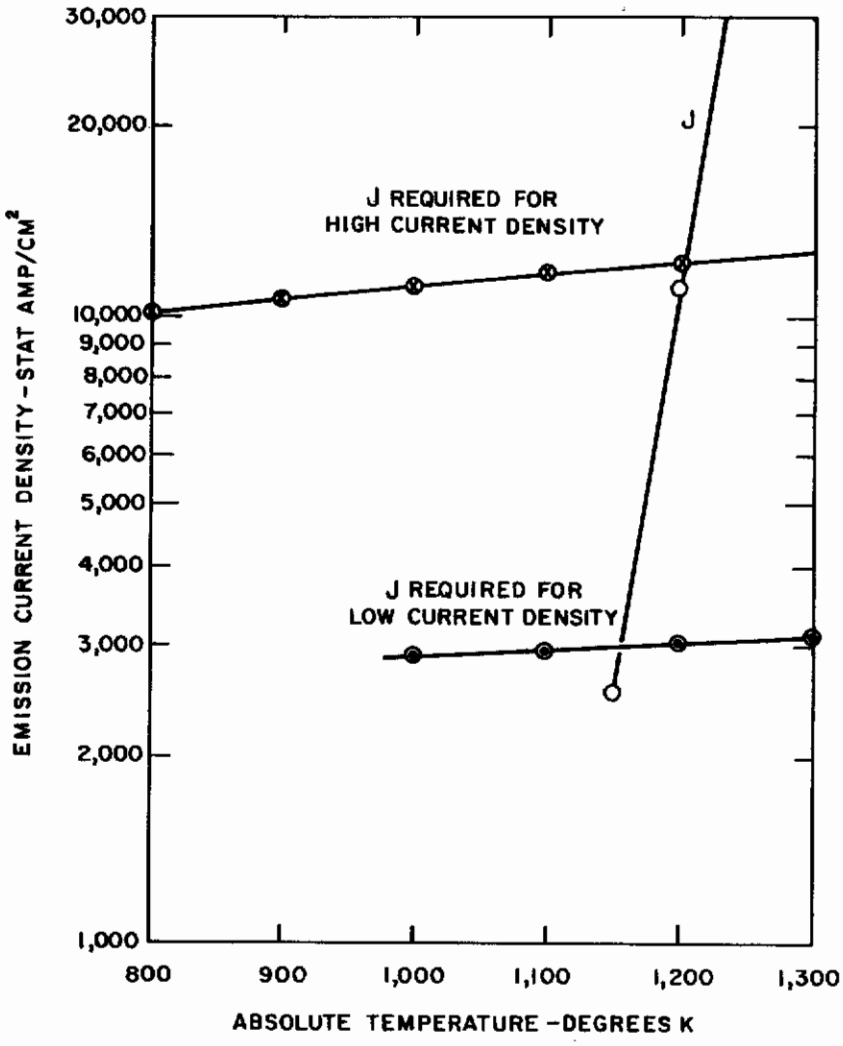

Figure 4. Graphic Computations of Steady-Source Temperature Required to Yield the Necessary Thermionic Emission of Li^+ Ions

B&S #40 wire, at 2-cm spacing, operating at 880°C (0.5 watt/cm^2 heating power density) and having a field strength of 41 esu at the wire surface (12.3 kv/cm). Because of the small radius of the wires, the region of high field strength and high temperature is confined to a small fraction of the total volume; this region is also far removed from the reaction volume. A potential drop of approximately 1.2 stat volts (360 volts) exists between the grid and the cathode under these low current density conditions.

Compromise of Design to Meet Other Requirements

Further modifications of the ion source design were imposed to facilitate fabrication. The final result was to increase the spacing to 3.5 cm, giving a 10-wire grid for a 35x35-cm cell. The reduction of the area of the opposing collecting electrodes to somewhat less than 10% of the total area available ($\sim$100 cm^2) to suppress diffusion increased the necessary potential drop by a factor of 10, $\sim$ 3.6 kv. This 35x35-cm cell should handle flows around 1 cm^3/sec of 1 ppm contaminant in air while drawing 8 μa of Li^+ ion current. Theory suggests somewhat less than 50% efficiency for such a cell. How much less depends mostly on the efficiency of the measures taken to suppress back diffusion.

Techniques of Fabrication

The wire alloy selected to support and heat the thermionic source was a nickel-chromium alloy sold under the name Tophet A for electrical heating service in air. It has high resistance to oxidation at temperatures to 1000°C. Its chief drawbacks for use in the present apparatus are a large temperature coefficient of expansion and a low tensile strength at high temperatures. Many of the difficulties encountered during development of the ion source stemmed from these properties of the substrates. However, the alloy is cheap, easily available in desired form (40-gauge wire), and resists corrosion.

Ion source wires were prepared by treatment in a series of solvents: (1) degreasing by trichloroethylene, (2) immersion in hot nitric acid, and (3) immersion in hot 50% acetic acid. This was followed by several washes with hot distilled water. A commercial process used to prepare nickel for oxide coating to form thermionic emitters of electrons in the electronic tube industry was followed for this treatment.

The wire was then coated with a slurry of lithium alumino silicate in thinned collodion lacquer. The lacquered wire was air dried and then oven dried at 150°C. After mounting the wire, the lacquer was fired off by passing current through the wire.

Spodumene was used in early work with these wires because it was the only lithium alumino silicate available at the time. Spodumene produced an ion source of limited life and emission. β-eucryptite was far superior. This material was synthesized by vacuum induction furnace fusion of pellets made from a ball-mill triturated mixture of lithium carbonate, hydrated aluminum oxide and hydrated silicon dioxide in the proper molar proporations. (The use of carbonates and hydrates caused considerable gas evolution during the fusion process. Hydrates were chosen because it was assumed that they would fuse with lithium carbonate more readily than would the oxides.) The resultant fused mass of eucryptite was ground to a powder in a ball mill. Test sections, prepared from 40-gauge wire coated with this powder slurried with lacquer, showed erratic performance with respect to Li^+ emission. Microscopic examination of the powder revealed that the average particle size was much too large, in comparison with wire's diameter, to achieve a uniform coat on the wire. Samples of the powder were then hand ground using a Mullite mortar and pestle and separated into coarse and fine fractions by selective sedimentation from aqueous suspensions. The cut off point was taken at 20μ, 25% of the 40-gauge wire's diameter. When applied to test pieces of support wire, the dried fine fraction gave much less erratic results than did the unground and unclassified β-eucryptite.

A brief attempt was made to identify unequivocally the positive ion emitted from these coated wires. For this purpose, the test apparatus described below was placed in a large vacuum desiccator flushed with a gentle stream of filtered prepurified-grade nitrogen. The ion current was collected on silver foil that had been washed and dried. After a measured ionic charge had been deposited on the foil, it was washed in 4% butyl alcohol and the washings analyzed for lithium. About 0.5 μg of lithium in excess of the blank was found. This was of the correct order of magnitude but about fourfold too large for a lithium equivalent of the measured charge transferred. The discrepancy may have been due to the considerable analytical uncertainty or to electrostatic precipitation of lithium-containing fume from the hot source. The latter thought discouraged further attempts at ion identification by this simple approach.

The preliminary tests described above used coated, 35-cm lengths of B&S #40 wire mounted on contiguous insulated terminals. The wire was pretensioned into a hairpin shape by a 10-gram weight on a wire over a terminal, functioning as a capstan. This hairpin wire was opposed by a 10x25-cm metal plate placed at a distance of 1 cm and set at a potential of -300 volts. Adjustable heating power was derived from the secondary winding of an isolation transformer with a grounded center tap. Ion current was measured by an electrometer inserted into the ground return from the polarizing 300-volt battery. Most tests were in ambient air. Emission of 0.5 μa or more, sustained for four hours, was regarded as satisfactory. This

emission per unit length of 0.015 μa/cm was equal to the emission required within the purification cell.

Convective Heat Transfer from Source

In the purification cell, a grid of ion source wires was placed 1 cm below a water-cooled metal plate in the cell (see below). Power dissipation was 0.4 watt/cm^2 of the water-cooled plate. A simple convective model of the heat transfer situation about the grid wires indicated that air would be heated to 400°C by these wires and would rise at velocities of a few centimeters per second toward the backing plate. It would then be cooled to near 30°C and fall back to the grid plane at a velocity around 1 cm/sec.

Ion Source Mounting Techniques

In mounting the fragile coated wires, the following factors were found to be important: (1) thermal expansion, (2) low tensile strength at high temperature, and (3) pitting corrosion of the alloy substrate in the presence of the hot alkaline eucryptite. The latter factor was confirmed by microscopic examination of the substrate for successful ion source tests. At 1000°C, the tensile strength of Tophet A wire drops below 10^4 psi, and the stress for 0.2% permanent set is below 5000 psi. This latter figure meant that tension had to be held somewhere below 17 grams for 40-gauge wire. How far below depended on the extent of pitting corrosion during the source service life of four hours. Pretensioning was necessary to take up sag due to the 5% expansion that occurred on heating to 1000°C. Various methods of mounting the wire grid in the cell were tried as a reliability test, taking advantage of increased probability for detecting random faults with a 10-wire arrangement. These tests with the complete cell (described below) were useful also for accumulating experience with the rest of the system at the same time. Initial tests were with designs that imposed 10 grams tension. This proved to be far too much tension, as the grid wires invariably broke within an hour after being placed in service. The initial tensioning device consisted of weak helical torsion springs with a relatively long straight arm leading from the free ends of the coils. The captive ends of the coils were soldered to Teflon-insulated, feed-through terminals in the water-cooled backing plate. The 40-gauge ion source heater wires were electrically spot-welded to the end of the free arm with the spring preloaded. A version using smaller diameter wire yielded torsion springs so weak that the grid wires could not be kept aligned in the same plane without extraordinary precautions. Hence, a redesign, became necessary. The new design consisted of very weak helical springs in extension, one end soldered to the feed-through terminals, the other spot-welded to the ion

source wire. These springs consisted of 20 turns (0.5-cm in diameter) of 0.016-cm diameter pure nickel wire. They exerted a tension ranging from 1 to 3 grams weight on the grid wires. The spring wire diameter was too small to carry the heating current which was bypassed around the spring. This pretensioning arrangement was fragile but gave a usable service life and was used during the significant experiments.

Section VI

CELL DESIGN

The final cell design, which incorporated all the features described above, with the exception of the ion source mounting method last discussed, was tested in mock-up form. Two trial dielectric materials were used--Plexiglass (an acrylate polymer) and Mycroy (a ceramic composite of glass and mica). A dielectric material was to be used to fabricate the rather complicated arrangement of cell-feed plenums and diffusion barriers in front of the porous collecting electrodes. The Plexiglass represented a mock-up of a plastic cell with Teflon-faced walls. Simulated collection electrodes were placed at the bottom of 0.4-cm wide by 1.0-cm deep slots in the test materials (simulating the diffusion barrier). Ten such slots approximately 30-cm long were selected for the final design. A simple shortened version of these slots were used in the mock-up. It was found that:

1. The use of Plexiglass led to temperature-dependent leakage currents, while Mycroy showed no such phenomena.

2. The wires of the ion source grid had to be directly over and close to ($\lesssim$0.5 cm) the slots in order to hold total potential drop below 3 kv (the maximum available from the polarizing supply) at the requisite ion current.

3. The ion-repulsive guide electrodes should not be immersed in dielectric if leakage currents of long relaxation time are to be avoided.

Based on these findings, the cell was designed as a sandwich of several machined Mycroy plates and spacers held together by two terminating metal structures, each layer sealed to the other by Viton O-rings retained in machined grooves in the Mycroy. A metal bottom piece consists of a flanged cover with a silicone gasket. This piece supports the bottom Mycroy plate and serves as a shield and support for electrical and gas connections to the cell bottom. A metal top piece consists of a machined stainless steel (304 ELC alloy) plate 0.95-cm thick that is an integral part of a proprietary heat exchange panel (Dean Products Panel Coil 301, single embossed, on a 3/8-in. thick back sheet with extended margins). The back sheet is milled flat and the extended margin of the sheet drilled and tapped to take the Teflon-insulated feed-through and mounting terminals, which support and feed power to the ion source grid 1 cm below the plate's interior surface. The 10 grid wires are on 3.5-cm centers. During cell operation, cold tap water is circulated through the embossed channels attached to this plate.

Three Mycroy sheets (called Sheets A, B, and C, for convenience) and one Mycroy spacer are sandwiched between the metallic top and bottom pieces. The lowest sheet (A) serves to mount the porous collection electrodes. The electrodes are brazed to the open sides of miniature stainless steel troughs embedded flush with the top surface of the 1.27-cm thick bottom sheet. Each trough is drained by a short piece of stainless steel tubing passing through the supporting Mycroy sheet to a plenum enclosed within the metal bottom piece. These drains also serve as electrical connections for the collection electrodes' polarizing power supply. The two upper sheets (B and C) have slots cut to match the electrodes.

Sheet B is 0.48 cm thick and is sealed to the electrode-support sheet (A) by a Viton O-ring. Machined into its lower surface are a shallow plenum and galleries that can feed a peripheral film of eluting air around the edges of each collecting electrode.

Sheet C is 0.48 cm thick and has plenum, galleries, and O-ring retaining grooves similar to Sheet B. The function of the plenum and galleries is to inject the incoming stream of contaminated atmosphere at a plane halfway up the diffusion barrier slots.

The 1.5-cm spacer's function is to hold the water-cooled 0.95-cm steel plate and the attached ion source grid at fixed distances from the collection electrodes. The spacer is in the shape of a rectangular frame that has two O-ring retaining grooves machined into its surfaces. The space between the top Mycroy sheet (C) and the steel plate afforded by this spacer gives room for the ion source grid mounting arrangement and an outlet manifold. This manifold consists of a plenum with 11 evenly perforated parallel ducts attached. These ducts lie between the diffusion guard slots. The main function of the manifold is to collect the purified atmosphere rising from the slots. An additional function is to repel positive ions that may drift into the space between electrodes. To accomplish this, the entire manifold is biased positively relative to the collecting electrodes.

Section VII

AUXILIARY SYSTEMS

Power Supplies

Polarizing voltages for the cell electrodes and heater current for the ion source are furnished by four regulated power supplies, two of which are high-current, low-voltage supplies connected in series to furnish heating power to the ion source grid. Their regulating circuits are connected in a master-slave mode to simplify adjustment of heating power. The circuit diagram of these interconnected supplies and their attachment to the ion source grid is shown in Figure 5.

The remaining supplies furnish polarizing voltages to the various electrodes within the purification cell. Several attempts are made to connect these voltage sources and an electrometer so that current to all electrodes could be measured. However, persistent leakage problems within the switching circuits, combined with a desire for economy, forced the adoption of a circuit which permitted measurement of the ion current at the collection electrodes only.

This circuit is shown schematically in Figure 6. The leakage current around the polarization power supply for the collector was measured at maximum voltage and found negligible in comparison with 1 μa--that is, the current returned to ground by this supply is due to the positive ions collected at the electrode. Operating voltages are -3000 volts on the collecting electrode and about -500 volts on the collection manifold. This latter voltage was adjusted for maximum collector current during each run.

Cell Flow Control

Flow of gases into and out of the purification cell is controlled by a system of stainless steel tubing, valves, and flowmeters. This system, shown schematically in Figure 7, mixes two metered streams of gas to form a flow of contaminated atmosphere from a stream of purified air and diluted contaminant in nitrogen. The excess flow, if any, may be discarded. A measured flow of the contaminated atmosphere may be directed into the purification cell or to analysis by flame ionization. If desired, a second stream of purified air may be metered into the cell to elute the porous collecting electrodes. A third stream of purified air may be directed to analysis to furnish a blank. The cell output consists of two streams: the purified stream, which is metered into the atmosphere, and the enriched stream, which can be discarded or analyzed at the experimenter's discretion.

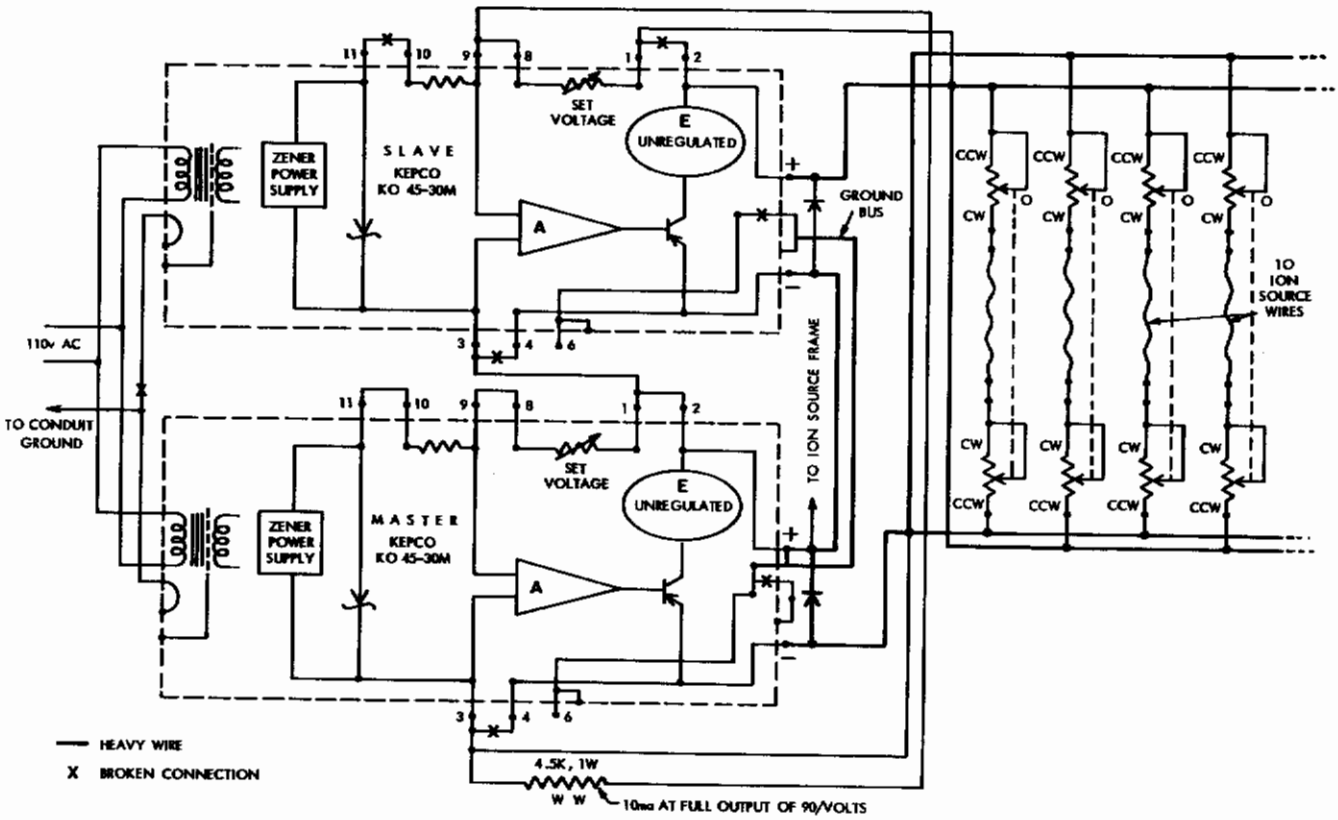

Figure 5. Schematic Diagram of Circuits, Ion Source

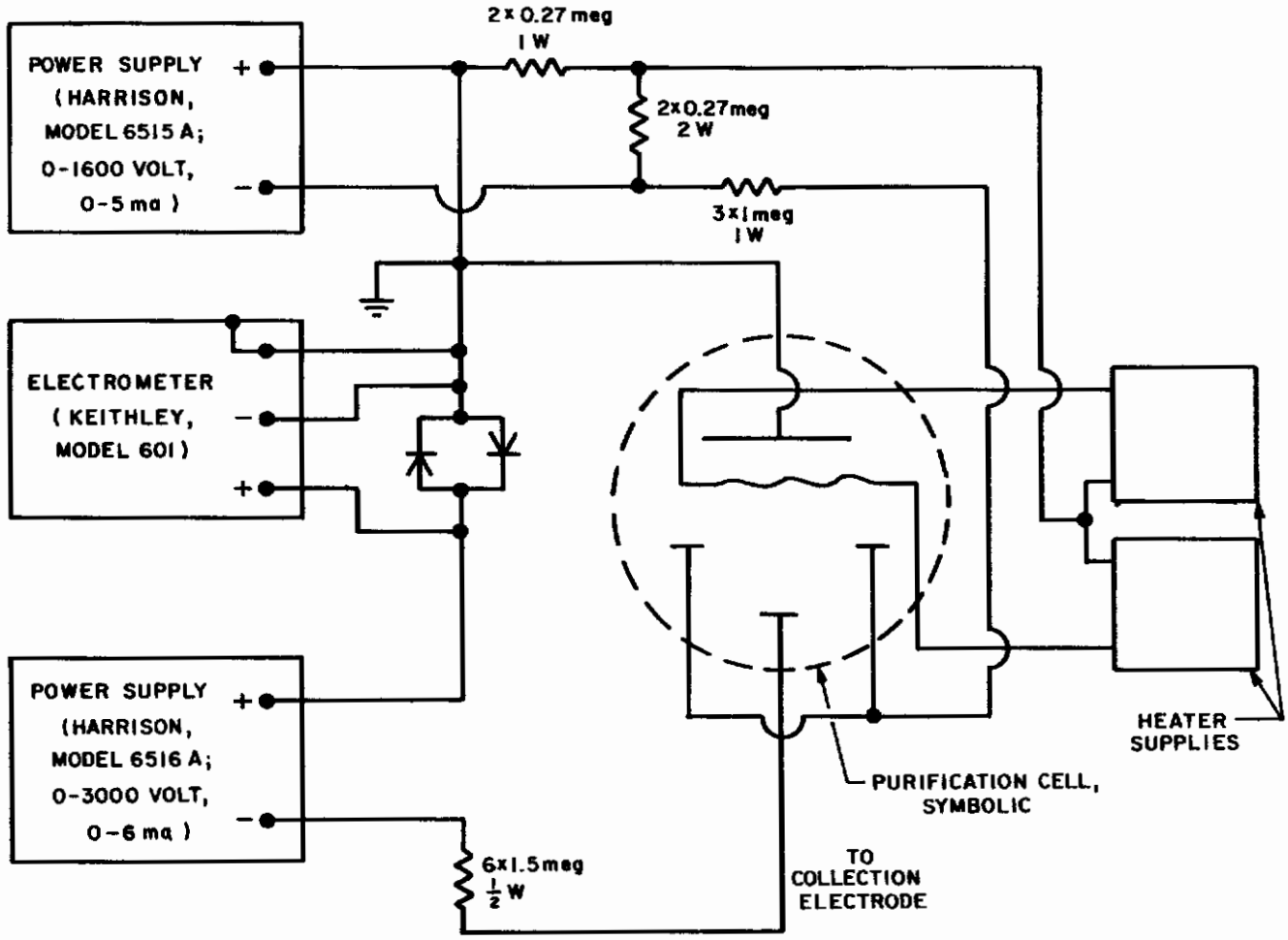

Figure 6. Polarization Circuits

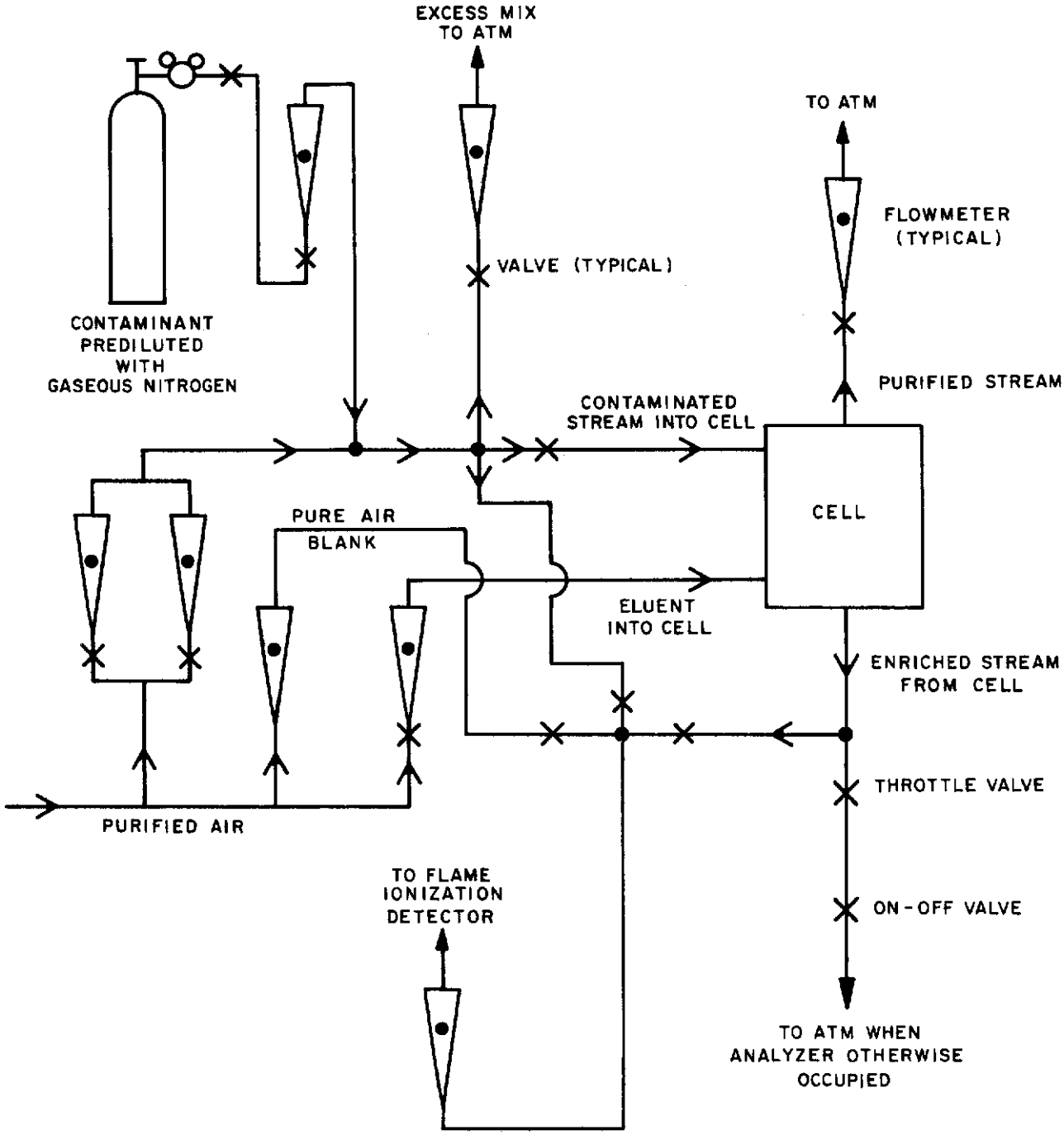

Figure 7. Schematic of Gas Flow Control System Feeding Purification Cells

This flow system is built up entirely of stainless steel, Teflon, Viton, and glass. (Earlier versions of this system having aluminum and anodized aluminum components were found completely unsuitable for use with acetone contaminated atmospheres because of sorption-desorption phenomena.) The present system, although usable, has relatively long relaxation times (of the order of an hour) on changing acetone concentration. This is attributed to the extremely dry carrier gases used in these experiments. Because of insufficient competition by water vapor, significant acetone adsorption takes place on internal surfaces, giving rise to adsorption-desorption effects.

Analysis for Acetone

Analysis for acetone in air is by hydrogen flame ionization using the modified detector unit of a GC (gas chromatograph, Aerograph Model 600) furnished with metered flows of "zero gas" (Matheson) hydrogen and air (flow rates 35 and 400 ml/min, respectively). The original electrometer and polarization voltage supply of the GC caused excessive noise and drift in the output signal. Therefore, the GC electrometer was replaced with a General Radio Electrometer (Type 1230A) used in the high input impedance (E-mode) configuration with its input shunted with a shielded low leakage 0.1-μf capacitor. At the input impedances used, this results in integrating time constants of 10 and 100 seconds and a usable signal-to-noise ratio. The output of the electrometer was recorded by a strip-chart recorder. The polarization voltage for the flame ionization unit is derived from a 300-volt dry battery.

Purification of Carrier Air

Air used as the carrier for contaminants is drawn from a compressed air supply at rates up to 1ℓ/min and thoroughly purified before being mixed with the prediluted contaminant. A schematic of the purification train is shown in Figure 8. The bulk of the polar and particulate impurities are removed by the filter and alumina tower. Catalytic combustion is used to oxidize any trace organic materials remaining to water and carbon dioxide. Experience with this type of furnace indicated that there may be, at most, 10 ppm (probably much less) nitrogen oxides added to the air by this catalytic treatment. Passing the air through a series of traps (see Figure 8) should reduce the concentration of carbon dioxide, water, and nitrogen dioxide to 0.1 ppm V/V or less. There may be, at most, a few parts per million of residual nitric oxide in the purified air stream. However, these estimates should be checked analytically.

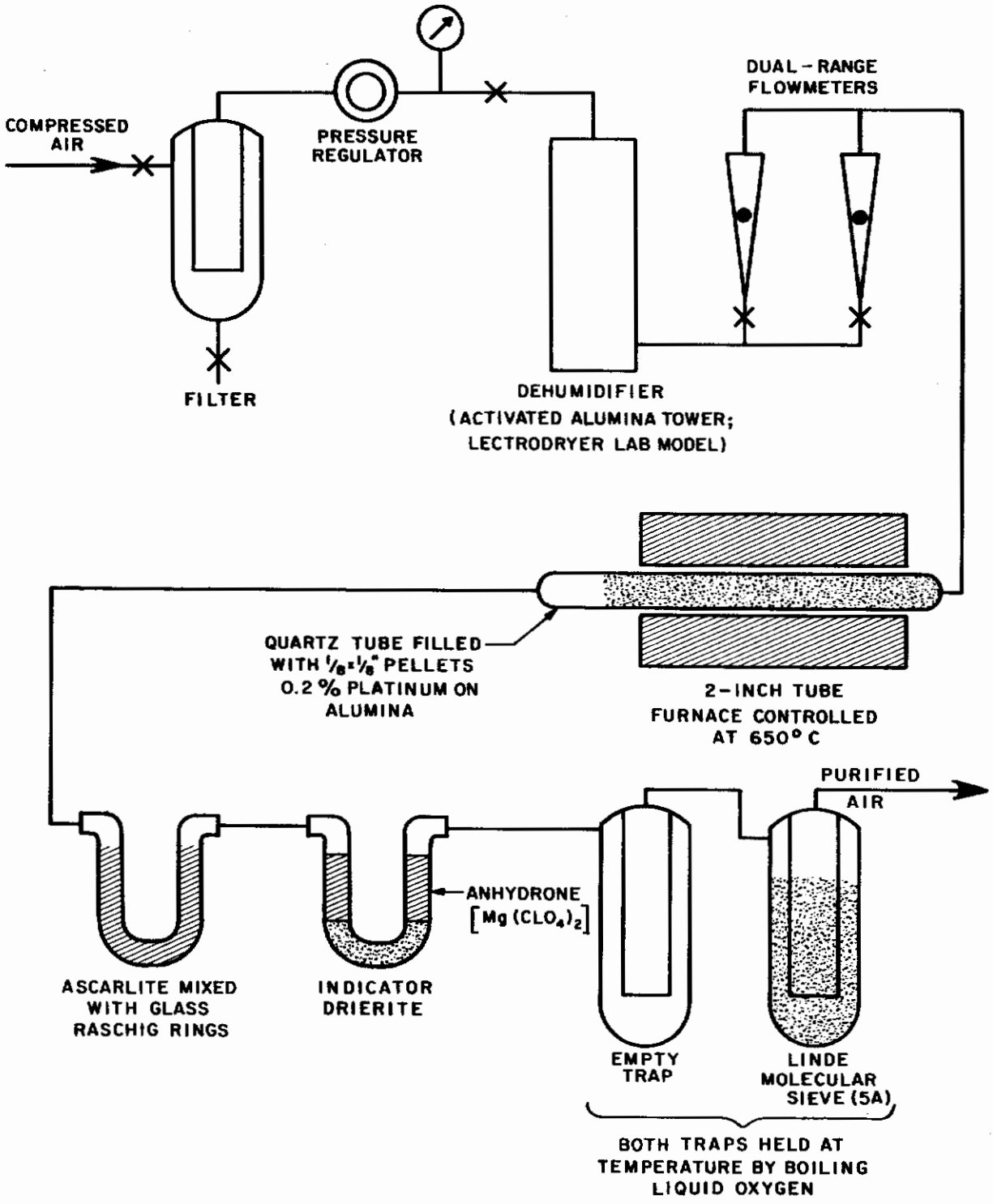

Figure 8. Schematic of Air Purification Train

Contaminant Source

The prediluted contaminant used was prepared by Scott Research Laboratories in a standard 2000 psig gas cylinder (17.3 ppm acetone, <5 ppm water, balance nitrogen). In future work, a system* consisting of a conventional vacuum system and a high pressure (~100 psig) filling line could be used for preparing tanks of prediluted contaminants.

---

* Three special stainless steel pressure tanks were built for use with this system. These tanks have two inlets, one vacuum and one high pressure. In use, the tanks are evacuated with baking to 1 μtorr and then filled with vapor of the contaminant to a measured pressure. The vacuum tank inlet is then closed and nitrogen is bled into the tank through the high pressure inlet until tank pressure reaches 100 psig. The diluting nitrogen is run through two stainless steel cold (LOX) traps, in series, which are packed with 5A Molecular Sieve. The purpose of these traps is to reduce the water content of the nitrogen.

Section VIII

EXPERIMENTAL RESULTS FOR ACETONE

Three experimental runs with acetone as the contaminants produced meaningful results. Two experiments gave a measured efficiency of removal of acetone of 20%. This is somewhat better than a theoretical estimate of 15% efficiency. It should be noted that this estimate was corrected for back diffusion partially suppressed by a separate eluting stream, which was not used.

Definition of Efficiency

In these experiments, steady-state concentration levels of acetone in the contaminated stream to and enriched stream from the purification cell (Figure 7) were measured without and with a positive ion current through the cell. The results are summarized in Table III. Efficiencies given were calculated in two ways:

$$\frac{(C_r - C_i)\, Q_r}{i \times 15.2}\ ,\ 15.2i \leq C_i Q_i \qquad (43)$$

where C_r = concentration of the enriched stream at steady state, ppm
C_i = concentration of the influent stream, ppm
Q_r = flow rate of the enriched stream, ml/min
Q_i = flow rate of the influent stream, ml/min
i = ion current, μa

and 15.2 is a numerical factor converting ion current to an equivalent acetone influx in the units (ppm x ml/min). The quantities calculated in this manner are the number of moles acetone removed per mole of Li^+ ion passed through the cell. This expression seems appropriate for those runs where the acetone is in excess relative to the ion current. When the ion current is in excess, another expression for efficiency seems more appropriate:

$$\frac{(C_r - C_i)\, Q_r}{C_i Q_i}\ ,\ 15.2i > C_i Q_i \qquad (44)$$

In both of these expressions the denominator constitutes the maximum possible removal corresponding to a 1:1 ratio of acetone molecules to Li^+ ions in a cluster.

Typical strip-chart data for one of these experiments, DMK-3, is sketched in Figure 9. Obviously, objective interpretation of the data is difficult, and further experiments are needed to confirm estimated efficiencies, thereby establishing confidence regions. Several replications normally are needed in work with trace concentrations; however, the project budget allowed no opportunity to perform blank or confirmatory experiments or experiments using a separate eluting stream. This latter mode of operation should enhance removal efficiency.

Table III

DATA ON REMOVAL OF ACETONE

Experiment Number	Contaminated Stream		Enriched Stream		Ion Current	Efficiencies[a]	
	Concentration (ppm)	Flow (ml/min)	Concentration (ppm)	Flow (ml/min)	(μa)	Referred to Current	Referred to Influx
DMK-1	1.4	100	5.6[b]	25	5.0	<1.38	<(0.75)
DMK-2	1.6	35	2.0	25	5.0	(0.13)	0.18
DMK-3	0.7	100	1.2	25	3.1	0.27	(0.18)

a. Efficiencies given in parentheses are inappropriate in the sense discussed in the text.

b. The ion source failed before steady state was achieved in experiment DMK-1; therefore, only upper limits can be quoted for efficiencies. This experiment was abnormal in one other respect, the ion source used was in an intermediate stage of development. The defect of this source is likely to have caused a very uneven distribution of ion current over the collecting surfaces.

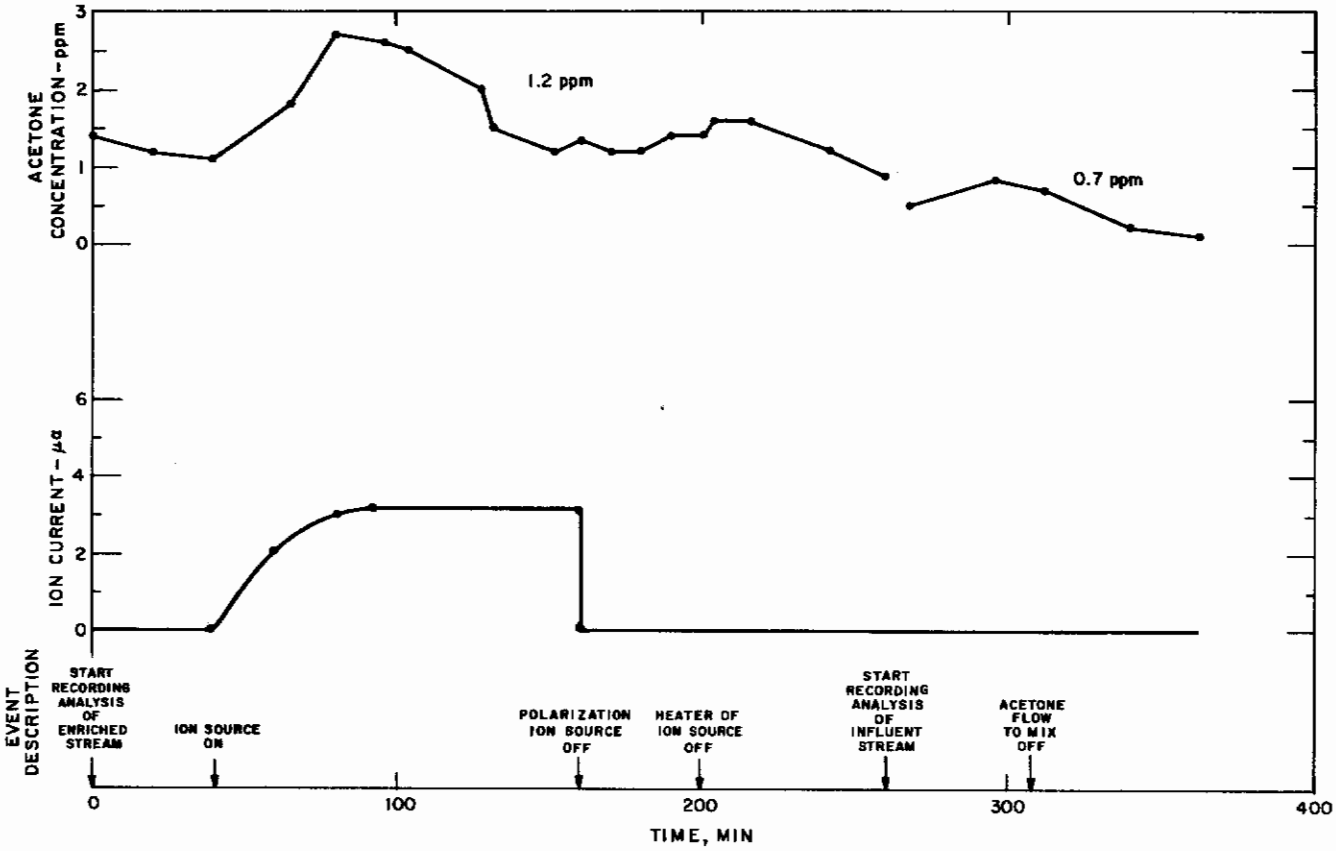

Figure 9. Typical Data from Strip Charts (Experiment Number DMK-3)

Section IX

PROPOSED FUTURE WORK

Apparatus Improvements

Extensive development work was required to bring the ion source to the stage of reliability required for the three experiments described in Section VIII. These meaningful experiments represent about two-thirds of those attempted. The major problems are associated with loss of strength of the grid wires. A more durable heating element material is needed; possibly the platinum alloys would be economical overall for this use.

The long relaxations and large sorption-desorption transients evident in Figure 9 are undesirable in that they increase the duration of an experiment. This increase, in turn, increases the probability of an aborted experiment and of experimental error due to drift. These effects probably can be reduced by decreasing the available surface area at the electrodes--that is, by using fine gauze instead of sintered metal. Also,the cell walls probably can be rendered less sorptive for polar compounds by coating with a thin film of Teflon.

It is recommended that the apparatus be improved in accordance with the above suggestions before further work is undertaken.

Further Work with Acetone

Additional experiments using acetone as a test contaminant need to be done. Such experiments would have three objectives: to confirm previously measured efficiencies, to investigate the possibility that non-ionic effects are contributing to the measured efficiency, and to investigate briefly methods of attaining greater efficiencies (within the limitations of the apparatus). After this series of experiments, other contaminants could be investigated.

Further Work with Other Contaminants

Experiments to establish a basis for estimating relative efficiency for any contaminant could be carried out. These would consist of standardized experiments using the low molecular weight members of three homologous series of widely differing polar properties. Methyl alkyl ketones, primary saturated alcohols, and saturated straight-chain hydrocarbons are suggested series.

REFERENCES

Allison, S. K. and M. Kamegai, "Lithium Ion Sources," Rev. Sci. Instr., 32 (10), 1090 (1961)

Blewett, J. P. and E. J. Jones, "Filament Sources of Positive Ions," Phys. Rev., 50, 464 (1936)

Cropton, R. W. and M. T. Elford, "The Mobility of Potassium Ions in Nitrogen and Neon at 294°K," Proc. Phys. Soc. (London), 74, 497 (1959)

Doyle, G. J. and R. G. Caldwell, Feasibility of Removing Gaseous Contaminants from Manned Space-Cabin Atmospheres by Ionic Processes, Stanford Research Institute, Final Report, Contract AF 33(615)-2405, with Wright-Patterson Air Force Base, February 1966

Green, A.E.S., Nuclear Physics, McGraw, New York, 1955

Kennard, E. H., Kinetic Theory of Gases, McGraw, New York, 1938, pp. 135-205

McDaniel, E. W., Collision Phenomena in Ionized Gases, Wiley, New York, 1964

Margenau, H., "On the Forces Between Positive Ions and Neutral Molecules," Philosophy of Science, 8, 603 (1941)

Massey, H.J.W. and E.H.S. Burhop, Electronic and Ionic Impact Phenomena, Oxford University Press, New York, 1952

Munson, M.S.B., "Reactions of Gaseous Bronsted Acids," J. Am. Chem. Soc., 87, 5313 (1965)

Munson, R. J. and K. Hoselitz, "The Mobility of Akali Ions in Gases: Part II. Attachment of Inert Gas Atoms in Alkali Ions," Proc. Roy. Soc., A172, 43 (1939)

Rubin, K., P. Dittmer, and B. Benderson, "Alkali 'Triode' Ion and Fast Neutral Source," Rev. Sci. Instr., 35, 1720 (1964)

Vedene'ev, Gurvitch, Kondrat'ev, Medvedev, and Frankevitch, Energii Razryva Khimicheskih Soyazei-Potentsialy Ionizatsit i Srodstro k Elektroniu, Akad. Neuk.SSSR, Moscow, 1962

Security Classification

DOCUMENT CONTROL DATA - R & D

(Security classification of title, body of abstract and indexing annotation must be entered when the overall report is classified)

1. ORIGINATING ACTIVITY *(Corporate author)*
Stanford Research Institute
820 Mission Street
South Pasadena, California 91030

2a. REPORT SECURITY CLASSIFICATION
Unclassified

2b. GROUP
N/A

3. REPORT TITLE
FEASIBILITY INVESTIGATIONS OF ELECTROSTATIC PRECIPITATION FOR THE REMOVAL OF GASEOUS TRACE CONTAMINANTS FROM MANNED CABIN ATMOSPHERES

4. DESCRIPTIVE NOTES *(Type of report and inclusive dates)*
Final Report 1 November 1966 - 31 May 1968

5. AUTHOR(S) *(First name, middle initial, last name)*
George J. Doyle

6. REPORT DATE
July 1968

7a. TOTAL NO. OF PAGES
44

7b. NO. OF REFS
13

8a. CONTRACT OR GRANT NO.
AF 33(615)-2405

b. PROJECT NO.
6373

c. Task No. 637302

d.

9a. ORIGINATOR'S REPORT NUMBER(S)
Stanford Research Institute Project No. SSU-5396

9b. OTHER REPORT NO(S) *(Any other numbers that may be assigned this report)*
AMRL-TR-68-111

10. DISTRIBUTION STATEMENT
This document has been approved for public release and sale; its distribution is unlimited.

11. SUPPLEMENTARY NOTES

12. SPONSORING MILITARY ACTIVITY
Aerospace Medical Research Laboratories
Aerospace Medical Division
Air Force Systems Command
Wright-Patterson Air Force Base, Ohio

13. ABSTRACT

This research is part of a program to study the feasibility of using a modified mode of electrostatic precipitation to remove polar gaseous trace contaminants from manned space-cabin atmospheres. A cell was developed for the removal of polar contaminant molecules from a 100 ml/min air inflow at part-per-million concentration levels of the contaminant. The operating principle of this cell is as follows: Positive lithium ions are thermionically generated and injected into the contaminated air stream. Ionic reaction products are collected at a set of porous metal collection electrodes. These electrodes are air-eluted. They are situated at the bottoms of slot-shaped wells to minimize escape of the collected contaminant molecules through diffusion. A measured efficiency of 20% for removal of acetone at a concentration of 1 ppm in dry air was finally achieved with this cell after considerable development work on the apparatus. This result is tentative pending further confirmatory experiments.

DD FORM 1 NOV 65 1473

Security Classification

Security Classification

14. KEY WORDS	LINK A		LINK B		LINK C	
	ROLE	WT	ROLE	WT	ROLE	WT
Experimental application of:						
Clustering about lithium ions: rates, equilibria						
Ion-molecule interactions						
Ionic processes						
To problems of:						
Purification of space-cabin atmospheres						
Removal of pollutants from air						
Air pollution						
Gas purification						
Air purification						
Pollution abatement						
Atmosphere purification						

Security Classification